China Geology 2 (2019) 142−156

China Geology

Journal homepage: http://chinageology.cgs.cn

Two types of uranium mineralization in Gulcheru quartzite: Fracture-controlled in Ambakapalle area and litho-controlled in Tummalapalle area, Cuddapah Basin, Andhra Pradesh, India

Sukanta Goswami[a,*], Pradeep Kumar Upadhyay[a], Bhaskaran Saravanan[a], V Natarajan[a], Mohan Babu Verma[b]

[a] *Atomic Minerals Directorate for Exploration and Research, Department of Atomic Energy, Bangalore* 560072, *India*
[b] *Atomic Minerals Directorate for Exploration and Research Department of Atomic Energy, Begumpet, Hyderabad* 500016, *India*

ARTICLE INFO

Article history:
Received 27 November 2018
Received in revised form 2 June 2019
Accepted 7 June 2019
Available online 12 June 2019

Keywords:
Uranium mineralization
Fracture-controlled mineralization
Litho-contralled mineralization
Gulcheru quartzite
Hydrothermal alteration
Andhra Pradesh
India

ABSTRACT

The Cuddapah Basin in southern India has a potential for uranium mineralization due to some favorable factors such as its temporal, stratigraphic and tectonic settings. Systematic exploration program conducted by the Atomic Minerals Directorate for Exploration and Research (AMD) within the Cuddapah Basin resulting in the recognition of distinct types of uranium mineralization, viz., strata bound type, fracture/shear-controlled type and tabular type. The Gulcheru Formation which is the lowermost unit of the Cuddapah Basin is dominantly arenitic in nature. During the exploration works, a number of uranium anomalies were identified with dimensions ranging from 1 m to 1.5 km. Gulcheru quartzite hosted uranium mineralization is intermittent and inconsistent in nature. The anomalous outcrops are distributed over a strike length of ca. 60 km between Gandi in the SE and Ambakapallein the NW. Presently, two different types of uranium mineralization are characterized on the basis of field observations, mapping and structural interpretation, petro-mineralogy and geochemistry. Although the host rock is same for both types, the mechanism of uranium enrichment is totally different. The Ambakapalle uranium mineralization is controlled by fault zone and associated hydrothermal activity. Whereas, the Tummalapalle uranium mineralization is litho-controlled in nature influenced by suitable four 'P' factors, i.e., provenance, porosity-permeability, precipitation and preservation. The geochemical characterization of Gulcheru quartzite suggest a passive margin type of provenance setting. Petro-mineralogically the quartz arenite suggests enough textural as well as mineralogical maturity. Ambakapalle quartzite is slightly strained and deformed due to faulting. Analysis of selected samples recorded 0.01% to 0.048% U_3O_8 and <0.01% ThO_2. Petrographic observation revealed that the anomalies were appeared due to secondary uranium minerals occurring as surficial encrustations, fracture filling and lesser irregular patches. Structural analysis suggests the mineralization along E-W trace slip fault is possibly consistent in sub-surface. Tummalapalle quartzite is relatively less deformed arenitic in nature with significant enrichment in MREE. The genetic models for the two types of mineralization is totally different.

©2019 China Geology Editorial Office.

1. Introduction

The Middle Proterozoic Cuddapah Basin has been the target for uranium exploration since 1950. This is a rifting associated sedimentary basin with remarkable types of uranium mineralization (Jayagopal AV and Dhana-Raju R, 1998; Rai AK et al., 2002; Parihar PS and Rao JS, 2012; Goswami S 2014; Goswami et al., 2017a). Systematic exploration activities in late 1980s have led to the discovery of strata bound type uranium mineralisation in phosphatic siliceous Vempalle dolostone of Papaghni Group of lower Cuddapah Supergroup in Tummalapalle area. This discovery of carbonate hosted uranium mineralisation which is syn-sedimentary in nature is unique in the world, . In addition to these following types of uranium mineralization in and around Cuddapah Basin, it forms a uranium province:

(i) Basement granite hosted fracture-controlled type.

(ii) Gulcheru quartzite hosted fracture and litho-controlled type.

(iii) Carbonate rock (Vempalle Formation) hosted strata bound type.

* Corresponding author: *E-mail address*: sukantoyahoo@gmail.com (Sukanta Goswam).

doi:10.31035/cg2018099
2096-5192/© 2019 China Geology Editorial Office.

Copyright 2019 Editorial Office of China Geology. Publishing services provided by Elsevier B.V. on behalf of KeAi.
This is an open access article under the CC BY-NC-ND License (http://creativecommons.org/licenses/by-nc-nd/).

(iv) Unconformity type between basement granite and Srisailam quartzite.

Presently, the Gulcheru Formation hosted uranium mineralization is the main topic of the paper. Gulcheru Formation is the lowermost stratigraphic unit of the Cuddapah Basin. This is dominantly quartz arenitic/ to wacke in nature and lying unconformably above basement granitoid complex. This unit hosts two different types of uranium mineralization viz, litho-controlled tabular style and fracture-controlled type. The Tummalapalle and Ambakapalle village areas are located in the SW marginal part of the Cuddapah Basin (Fig. 1). In fact, they belong to Papaghni sub-basin. Fertile uraniferous basement complex with dyke swarms is considered as the source and provenance. The two different styles of uranium mineralization indicate two different types of local geological setting up. Thus, geochemical characterization of host rock is prime objective for litho-controlled type Tummalapalle quartzite unlike the Ambakapalle area, where structural analysis is the main focus. Ambakapalle is situated at about 15 km NW of well-known Vempalle dolostone hosted

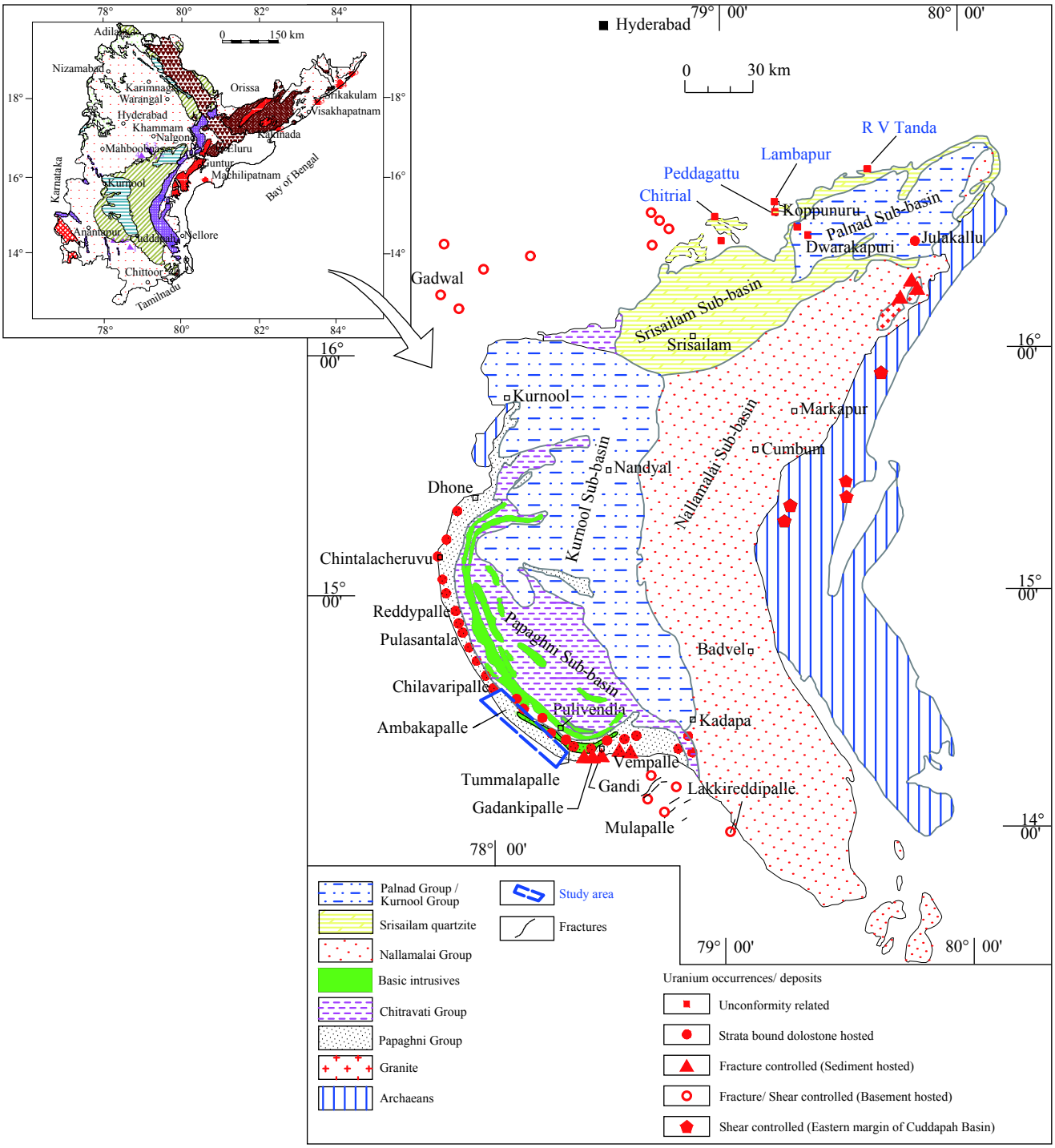


Fig. 1. Geological map of the Cuddapah Basin and its environs showing locations of uranium deposite and occurrences (modified from Geological Survey of India, 1981 and AMD Reports, Goswami, 2014).

Tummalapalle uranium deposit. However, in the present context Tummalapalle quartzite is our main objective.

2. Geological background

The crecent shaped Cuddapah Basin is situated in the east-central part of the Dharwar Craton and is the second largest Proterozoic, intra-cratonic, sedimentary Bbasins in India after Vindhyan. It covers an area of around 44000 km^2 and extends for a length of about 450 km along the arcuate eastern margin with a mean width of 150 km. The Basin is characterised by quartzite-shale-carbonate cycles and the early sediments of the basin are interspersed with basic volcanic and sills. Several works are done in the basin since eighteen seventies. Systematic mapping by Geological Survey of India (1981) led to some significant changes in stratigraphy. The intra-cratonic rift related Cuddapah basin comprises of Cuddapah Supergroup followed by Kurnool Group of sedimentary rocks. The Cuddapah Supergroup is developed in Papaghni, Nallamalai and Srisailam sub-basins whereas Kurnool Group occur in the Kurnool and Palnad sub-basin. The lowermost arenaceous Gulcheru Formation of the Papaghni sub-basin is our target in this context. The geology of Cuddapah Basin, stratigraphy and geological setup of Gulcheru Formation, was already discussed by several authors (Nagaraja Rao BK et al., 1987; Ramakrishnan M and Vaidyanadhan R, 2008) and references therein. Therefore, local geology of the study area is described in more detail.

The granitoids surrounding the S-W basin margin area are of two types: (1) Dark grey coloured coarse grained hornblende-biotite granite with feeble N-S gneissosity at places occupying relatively flat pane planed areas shows up to 0.02 mR/h activity and (2) medium to coarse grained granodiorite of pink to pinkish grey colour found in hillocks intruded over the earlier. This pink granodiorite occurs as plutons and gives higher radioactivity ranging from 0.04 mR/h to 0.06 mR/h. Several fracture trends are marked along E-W, NE-SW and NW-SE and N-S directions. Quartz reefs are also remarkable intrusive features which are found mostly along NW-SE, NE-SW and WNW-ESE trends. Hematitisation is noted near the contact zones of quartz reef and basement granitoids at some places. Basic intrusives with occasional porphyritic texture bearing intrusives are common.

A broadly E-W fault zone is located at around 2 km WNW of Ambakapalle area. The detailed map, section and satellite image is shown in Fig. 2–Fig. 4. Significant uranium mineralization was noted during the year of 2001–2002 with a grade of 0.13% U_3O_8 over a strike length of about 500 m and a thickness of up to 20 m along the scarp fractured face in Gulcheru quartzite. The strike of bedding plane is N40°W with a dip of 10° due NE with steeper dip near fault plane. The mineralized quartzite is very hard, massive and compact. The fracture has played a role for remobilization and concentration of uranium.

The location of study area around south of Tummalapalle area and the collected samples from uranium anomalies are shown in map and satellite image, respectively (Fig. 5–Fig. 6). This have given a clear evidence for litho-controlled nature since the mineralization, which occurs all along the bedding plane which is same as topographic slope in the area. Field observations suggests that the anomalies are located along bedding plane and ranges in dimension from 1 m×1 m to 50 m×10 m with values ranging from 5 mR/h to 0.025 mR/h. Presence of the secondary uranium minerals are very common and can be observed by unaided naked eye also.

3. Research methods

Systematic field traverses are taken along the entire study area. Structural analysis has been carried out around the fault/fracture zones. The time stratigraphic relationships of the Ambakapalle uranium mineralization is matching with Lower to Middle Proterozoic sub-unconformity epimetamorphic type (Dahlkamp FJ, 1993). The structural analysis was carried out during detailed geological mapping of the fracture zone located at around 2 km WNW of Ambakapalle village. The detailed mapping (Fig. 3) with the help of tape, compass and GPS readings were minutely cross checked for all the locations. All the litho-contacts were traced along with fracture trends and plotted in the map. Several narrow linear

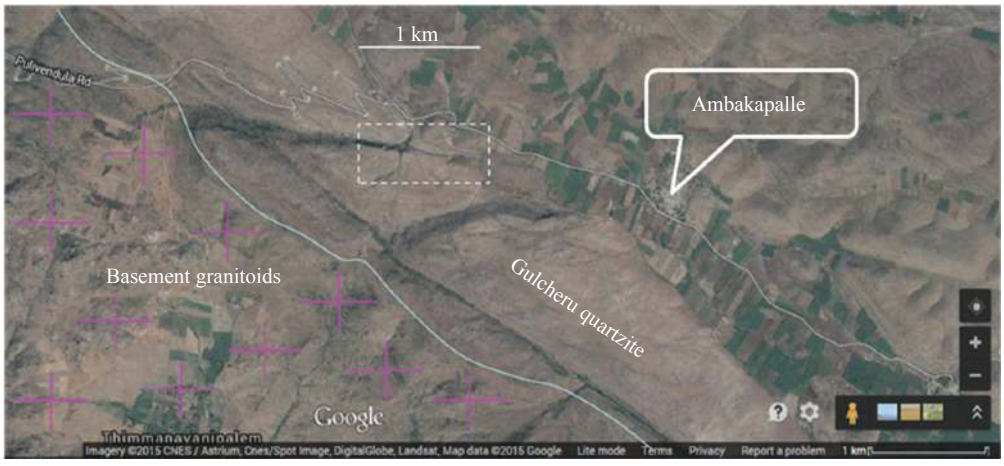


Fig. 2. Google image showing the study area, west Ambakapalle village, India.

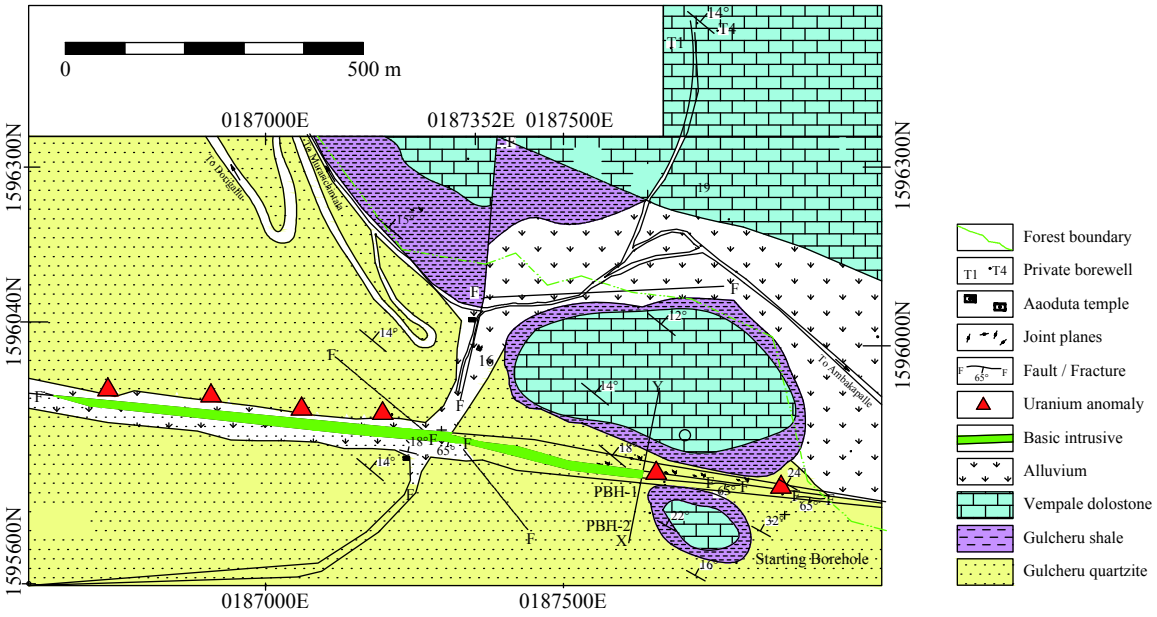


Fig. 3. Geological map of Ambakapalle area showing uranium anonalies, Kadap district, Andhra Pradesh, India.

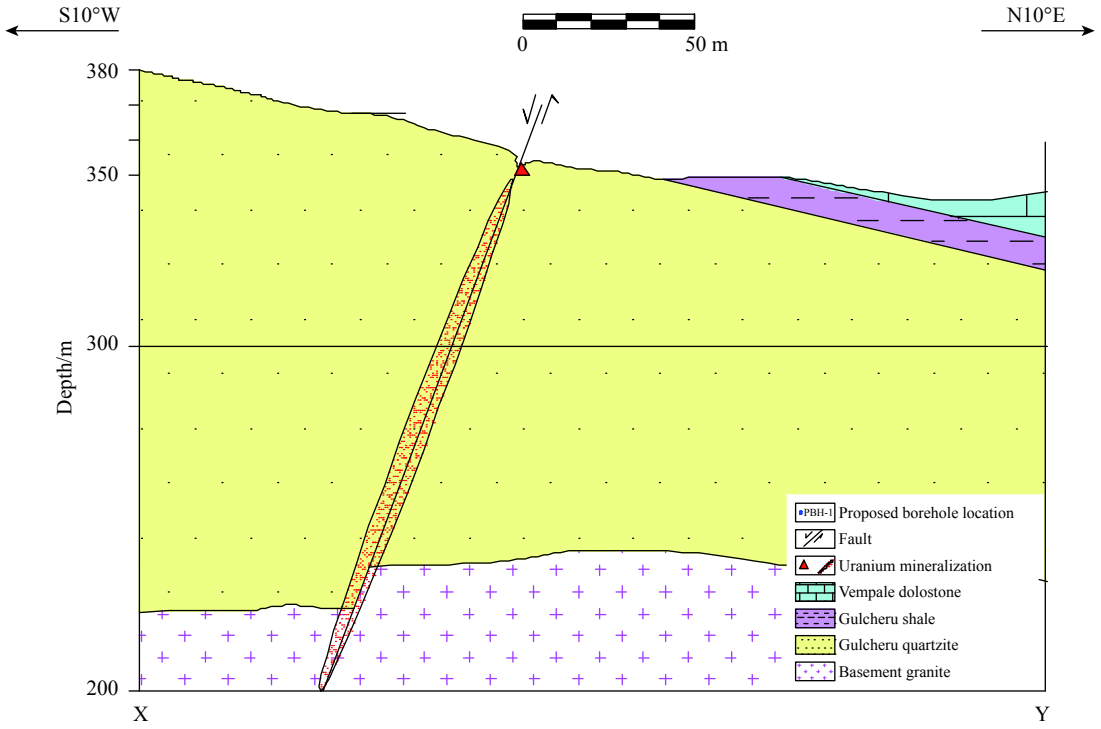


Fig. 4. Hupothetical section along X-Y (Fig. 3) showing probable subserface mineralization.

water channels (nala) have been developed due to intense fracturing and faulting and along those nala huge amount of broken brecciated pieces of quartzite boulders are transported and spreaded over shale. Total 13 samples of Gulcheru quartzite from Ambakapalle area were studied by XRF analysis and 28 samples were analysed for physical radiometric assay. Solid state nuclear tract detection (SSNTD) studies on the thin sections have also been carried out along with petro-mineralogical studies of selected samples.

20 representative samples of Gulcheru quartzites were collected from fresh outcrops along and across the strike direction from Tummalapalle area. Whole-rock chemical analyses were carried out at the chemistry laboratories AMD, SR, Bangalore. The analytical precession is better than 5% for major and trace elements. REE concentrations were determined by ICP-OES (Inductively Coupled Plasma Optical Emission Spectrometry). Pallet fluorometry was used for uranium. The thorium, vanadium, molybdenum, barium, strontium etc. were analysed by ICP-OES along with Al_2O_3, MnO, CaO, MgO. UV-visible spectrophotometery were used

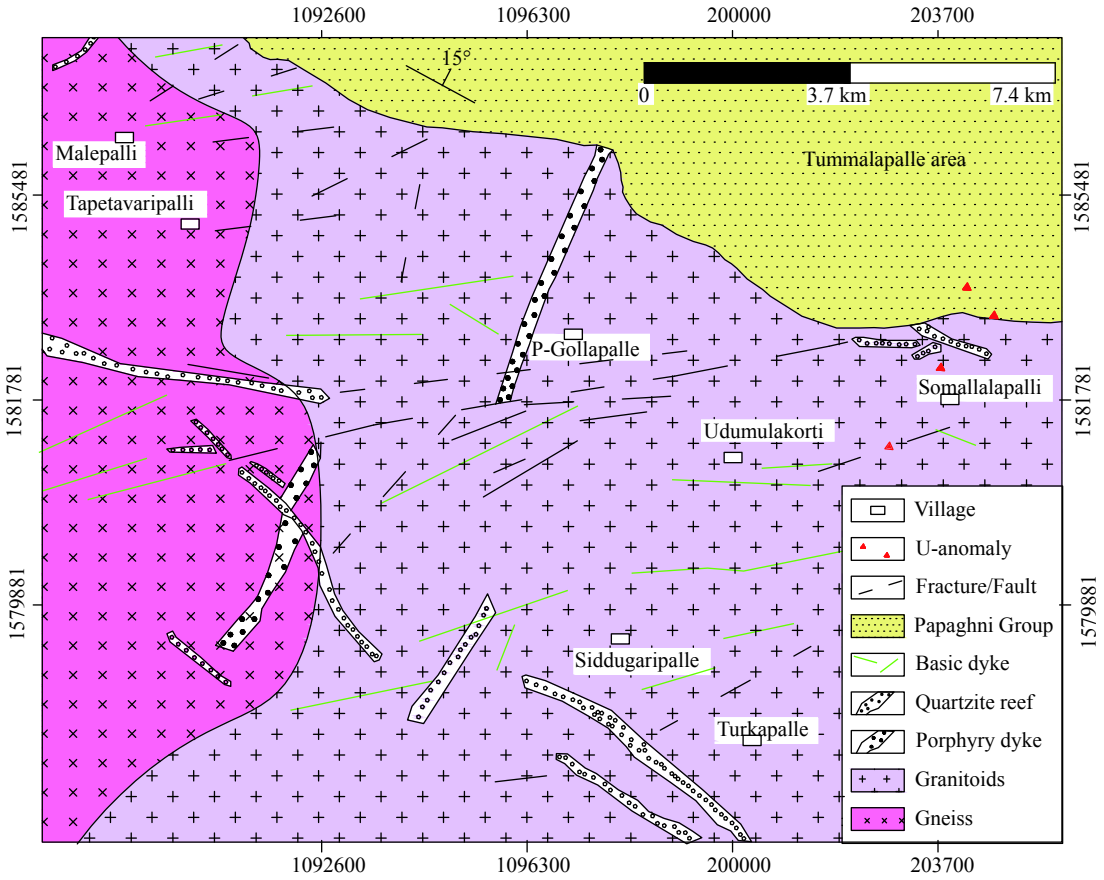


Fig. 5. Geological map of the area around Tummalapalle-Tapetavaripalle showing the study area at the south of Tummalapalle mine.

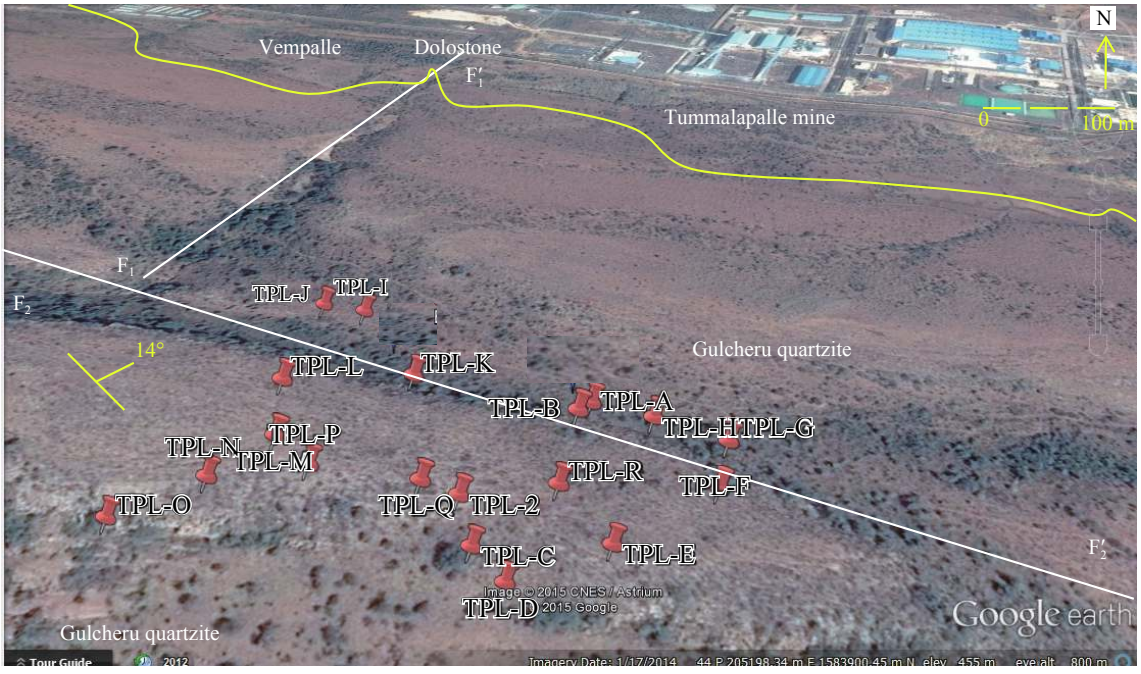


Fig. 6. Regional satellite image of sample points with UTM coordinates. The points show the strike and dip extent of uranium anomalies and demarcate lithocontrolled nature of mineralization in Gulcheru quartzite. The occurrence of uranium anomalies along ESE-WSW fracture zone is is coincidentally cut section. The anomalies near the fracture are noted as scarp face and this section in the south of Tummalapalle uranium mine is not indication of fracture controlled mineralization. Red pins (TPL-A, TPL2 etc.) are indicating uranium anomalies irrespective of structure.

for SiO_2, P_2O_5. Na_2O and K_2O were analysed by flame photometer. Trace elements like Cu, Ni, Co, Pb, Zn, Rb were analysed by AAS (Atomic Absorption Spectrometry). XRD analysis also have been carried out for identification of radioactive and other minerals after thin section studies under petrographic microscope which could not identified different secondary uranium minerals.

4. Results

The geochemical characterization of host rock around Tummalapalle area is very significant. On the other hand, structural analysis of the fault zone around Ambakapalle area is another important task. Table 1, Table 2 and Table 3 show the major and trace element data generated from the Tummalapalle quartzite samples. The objective to determine the palaeotectonic setting of provenances based on geochemical signatures of uraniferous Gulcheru quartzite near Tummalapalle uranium mine area has been substantiated in the present context. Average SiO_2 content of the Gulcheru quartzite in the area is more than 90% and consists of detrital quartz with limited amounts of other framework grains

Table 1. Major element oxide data (%) of Gulcheru quartzite samples, Tummalapalle area.

Sample No.	SiO_2	TiO_2	Al_2O_3	Fe_2O_3	FeO	MnO	MgO	CaO	Na_2O	K_2O	P_2O_5	LOI	U_3O_8(T)
TPL-A	84.57	0.05	4.10	2.76	2.09	0.02	2.80	0.15	0.10	0.21	0.20	2.09	0.002
TPL-B	76.82	0.02	1.60	17.90	0.74	0.02	0.09	0.17	0.09	0.07	0.35	1.30	0.014
TPL-C	95.03	0.04	1.87	0.26	0.37	0.02	0.23	0.26	0.03	0.40	0.15	0.79	0.002
TPL-D	89.78	0.03	1.81	0.20	0.43	0.01	0.18	3.70	0.05	0.50	2.40	0.32	0.001
TPL-E	90.94	0.05	2.08	3.43	0.69	0.02	0.10	0.21	0.03	0.15	0.20	1.16	0.013
TPL-F	85.50	0.05	2.23	3.46	0.63	0.01	0.16	3.30	0.05	0.24	2.50	1.04	0.016
TPL-G	91.44	0.03	2.30	1.44	1.03	0.01	0.30	0.29	0.03	0.04	0.30	1.12	0.011
TPL-H	95.62	0.02	0.70	0.45	1.02	0.02	0.85	0.10	0.02	0.02	0.10	0.84	0.086
TPL-I	90.97	0.04	1.89	1.63	0.88	0.02	0.59	0.25	0.03	0.06	0.25	1.44	0.541
TPL-J	81.61	0.05	2.70	1.38	0.58	0.03	0.85	6.20	0.10	0.25	4.20	1.15	0.011
TPL-K	96.30	0.03	1.08	0.11	0.57	0.01	0.07	0.04	0.01	0.50	0.10	0.28	0.003
TPL-L	90.70	0.07	2.78	0.29	0.64	0.01	0.20	1.14	0.07	0.69	0.85	0.73	0.008
TPL-M	94.25	0.04	1.52	0.67	0.83	0.01	0.10	0.07	0.01	0.24	0.30	0.65	0.417
TPL-N	95.10	0.03	0.95	0.20	0.59	0.01	0.13	0.11	0.02	0.20	0.20	0.61	0.137
TPL-O	95.26	0.04	1.94	0.10	0.50	0.01	0.20	0.21	0.03	0.50	0.15	0.58	0.001
TPL-P	94.89	0.03	0.82	0.19	0.47	0.01	0.06	0.41	0.02	0.15	0.55	0.48	0.334
TPL-Q	95.45	0.03	0.98	0.02	0.61	0.01	0.06	0.03	0.02	0.25	0.20	0.42	0.005
TPL-R	91.76	0.10	3.47	0.95	0.77	0.02	0.18	0.08	0.05	0.57	0.30	1.16	0.021
TPL-1	90.89	0.05	2.08	2.78	0.5	0.04	0.15	0.15	0.08	0.04	0.22	1.58	0.108
TPL-2	94.46	0.03	0.96	0.84	0.43	0.04	0.14	0.26	0.03	0.06	0.06	0.89	1.13

Table 2. Selective trace element oxide data (10^{-6}) of Gulcheru quartzite samples, Tummalapalle area.

Sample No.	Ba	Cu	Co	Ni	Rb	V	Cr	Sr	Th	Zr	Nb
TPL-A	65	100	25	60	<10	30	70	<10	<10	100	<10
TPL-B	75	250	40	170	<10	160	200	15	<10	50	<10
TPL-C	95	15	10	<10	<10	20	75	10	<10	65	<10
TPL-D	175	20	<10	<10	<10	10	65	<10	<10	140	<10
TPL-E	85	15	<10	10	<10	35	70	15	<10	50	<10
TPL-F	85	20	25	20	<10	35	60	30	<10	75	<10
TPL-G	75	145	10	15	<10	20	70	25	<10	50	<10
TPL-H	165	180	10	10	<10	10	55	<10	<10	25	<10
TPL-I	45	680	20	40	<10	35	70	<10	<10	45	<10
TPL-J	120	65	10	25	<10	30	60	40	<10	135	<10
TPL-K	65	25	<10	10	<10	10	65	<10	<10	30	<10
TPL-L	120	25	<10	<10	<10	20	75	20	<10	65	<10
TPL-M	85	30	10	15	<10	15	60	20	<10	30	<10
TPL-N	95	25	<10	<10	<10	10	60	10	<10	25	<10
TPL-O	80	15	<10	<10	<10	10	65	10	<10	35	<10
TPL-P	215	25	<10	<10	<10	<10	55	55	<10	25	<10
TPL-Q	65	25	<10	<10	<10	<10	65	<10	<10	30	<10
TPL-R	365	30	10	<10	<10	30	70	110	<10	90	<10
TPL-1	130	20	<10	60	<10	30	105	12	<10	75	<10
TPL-2	95	20	30	60	<10	15	90	9	<10	25	<10

Table 3. REE data (10^{-6}) of Gulcheru quartzite samples, Tummalapalle area.

Sample No.	La	Ce	Pr	Nd	Sm	Eu	Gd	Tb	Dy	Ho	Er	Tm	Yb	Lu	Sc	Y
TPL-A	<5	<5	<5	<5	<5	1.0	<5	<3	<2	<2	<3	<2	<1.0	<1.0	2	7
TPL-B	339	455	41	124	26	5.0	16	4	14	2	5	<2	2.8	<1.0	1	33
TPL-C	19	30	<5	16	<5	<1.0	<5	<3	2	<2	<3	<2	<1.0	<1.0	1	11
TPL-D	<5	8	<5	12	6	1.1	10	<3	9	2	4	<2	3.4	<1.0	1	36
TPL-E	<5	5	<5	5	<5	<1.0	<5	<3	4	<2	<3	<2	1.0	<1.0	2	11
TPL-F	5	11	<5	17	15	2.8	18	4	15	2	5	<2	2.8	<1.0	3	38
TPL-G	6	12	<5	10	<5	<1.0	<5	<3	4	<2	<3	<2	1.4	<1.0	2	17
TPL-H	<5	4	<5	6	<5	<1.0	6	<3	7	<2	4	<2	1.5	<1.0	1	17
TPL-I	5	24	7	29	29	5.2	42	11	46	7	17	2	7.9	<1.0	2	131
TPL-J	<5	5	<5	<5	15	3.7	21	5	19	3	7	<2	4.0	<1.0	4	77
TPL-K	9	15	<5	7	<5	<1.0	<5	<3	2	<2	<3	<2	<1.0	<1.0	1	4
TPL-L	<5	10	<5	9	5	1.0	5	<3	5	<2	<3	<2	1.2	<1.0	2	19
TPL-M	<5	10	5	22	21	4.3	27	8	31	5	12	2	5.8	<1.0	5	92
TPL-N	12	21	<5	13	5	1.0	22	7	34	6	15	2	8.1	1.0	1	176
TPL-O	20	34	6	19	<5	<1.0	<5	<3	<2	<2	<3	<2	<1.0	<1.0	1	4
TPL-P	9	17	7	24	19	4.7	48	12	51	9	21	3	11.2	1.3	1	222
TPL-Q	10	15	<5	7	<5	<1.0	<5	<3	2	<2	<3	<2	<1.0	<1.0	1	5
TPL-R	9	27	5	39	29	5.5	59	13	56	10	20	2	9.7	1.3	3	253
TPL-1	<5	22	<5	29	28	38.9	255	54	349	61	132	16	65.8	<1.0	1	1844
TPL-2	<5	7	<5	14	20	9.1	32	6	28	4	10	<2	4.3	<1.0	1	84
Comp	0.340	0.910	0.121	0.640	0.195	0.073	0.260	0.047	0.300	0.078	0.200	0.032	0.220	0.034		
PASS	38.200	79.600	8.830	33.900	5.550	1.080	4.660	0.774	4.680	0.991	2.850	0.405	2.820	0.433		

(feldspar, lithic fragments etc.) and matrix which suggests the term quartz arenite for the litho unit in the study area. However, though often diagentically fused grains are seen to classify these as quartzite, regionally very low to negligible degree of metamorphism supports to categorise this as quartz arenite which is highly mature texturally as well as mineralogically. At places arenite is cemented to quartzite, the individual quartz grains recrystallize along with the former cementing material to form an interlocking mosaic of quartz crystals and grainy, sandpaper-like surface becomes glassy in appearance. Since quartzite is very resistant to chemical weathering it has formed ridges and resistant hilltops in the area as capping over granitoids. The nearly pure silica content of the rock provides no soil. Therefore, the quartzite is bare or covered only with a very thin layer of soil and very little vegetation. It is known that various factors like the composition of source rocks, environmental parameters (e.g., atmospheric chemistry, temperature, rainfall and topography) influencing the weathering of source rocks, duration of weathering, transportation mechanisms of clastic material from source region to depocenter, depositional environment (e.g., marine, fresh water), and post-depositional processes (e.g., diagenesis, metamorphism) controls mineralogical and chemical composition of clastic sedimentary rocks. According to the XRD analysis of the uranium bearing samples are composed of mainly quartz and traces of albite and muscovite with secondary uranium minerals like uranophane [$Ca(UO_2)_2(SiO_3)_2(OH)_2{\cdot}5H_2O$], saleeite [$Mg(UO_2)_2(PO4)_2{\cdot}10H_2O$] and bayleyite [$Mg_2(UO_2)(CO_3)_3{\cdot}18H_2O$]. Several studies have been focused on the identification of palaeotectonic settings of provenances based on geochemical signatures of siliciclastic rocks (e.g., Dickinson WR and Suczek CH, 1979; Bhatia MR, 1983; Bhatia MR and Crook KAW, 1986; Roser BP and Korsch RJ 1986, 1988; McLennan SM and Taylor SR, 1991).

The effects of Eastern Ghat orogeny (ca.1570 Ma) is known fact for the development of the Eastern Ghats Mobile Belt (EGMB) in the east of the Cuddapah Basin. This deformation episode is the reason of the crescent shape of the basin. Near the western margin of Cuddapah Basin tectonic imprints of the EGMB is manifested as E-W faults at Ambakapalle area. The Ambakapalle quartzite is arenitic in nature comprises of about 95% quartz (of 0.4 mm to 0.5 mm) and few chert clasts also present as minor phase. Subrounded to subangular quartz clasts with sutured grain margins often show mild strain effects in the form of medium undulose extinction. Biotite and muscovite are also present in the matrix whereas heavy minerals like tourmaline and zircon are present as inclusions in the quartz clasts. Iron oxides like limonite and goethite are found the interstitial spaces and also as disseminated grains in matrix. SSNTD result indicated presence of adsorbed uranium. The chromogram test on the polished sample surface showed positive result and brown coloured spots were noted on photo paper (Fig. 7a, b). Only sparse to low density alpha tracks are noted after 4 days of exposure of cellulose nitrate (CN) film. The source of radioactivity is adsorbed uranium on anatase and goethite. These are present as disseminated grains in the matrix part of the rock (Fig. 7c, d).

4.1. Geochemistry of host rock

Unlike the Tummalapalle area, geochemical study in Ambakapalle area is used in a different context. The

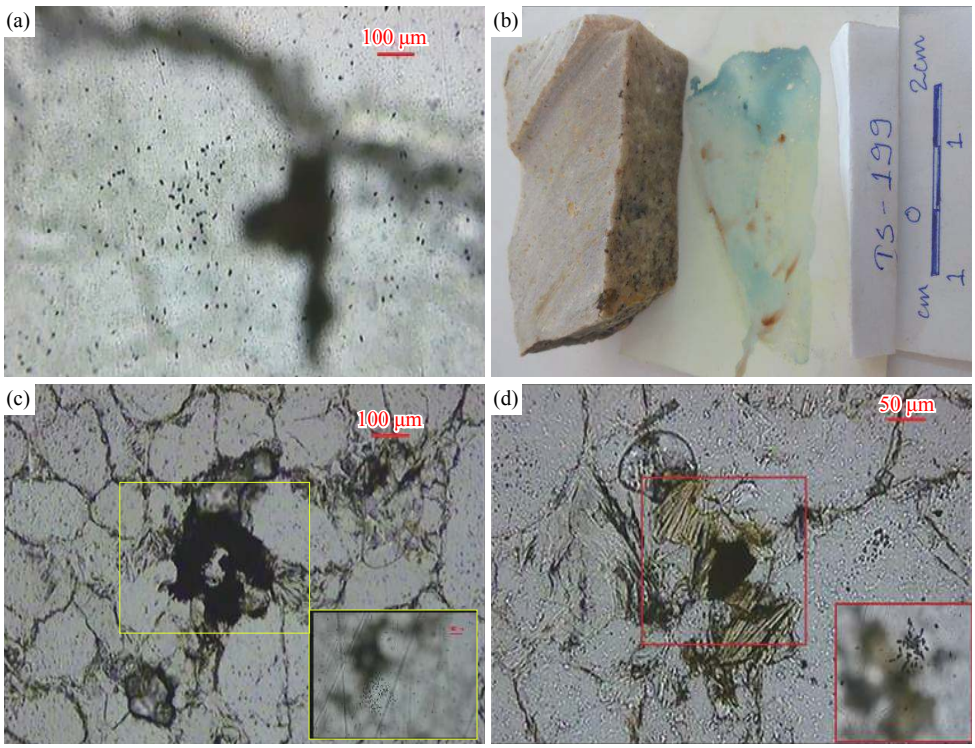


Fig. 7. Petrographic observation of Gulcheru quartzites from Ambakapalle area. a–Adsorbed uranium on goethite giving sparse alpha (α) tracks 10X, TL, 1N; b– positive chromogram test indicate presence of leachable uranium with characteristic brownish colour; c–adsorbed uranium on goethite with inset of sparsealpha tracks 20X, TL, 1N; d–adsorbed uranium on anatase with inset of sparse alpha tracks 20X, TL, 1N.

geochemical association of some trace elements like Sr, Ba in Ambakapalle give clues towards hydrothermal mineralisation because they are linearly varying with uranium. Even depletion of some compatible elements like Ni, Cr is indirectly indicating presence of late-magmatic hydrothermal fluid (Fig. 8). It can be noted that Rb do not show any correlation with uranium but strontium shows positive correlation with uranium. This is implies that apart from Rb some other hydrothermal source might have enriched Sr and hence linearity with U_3O_8. Different types of alteration indices are plotted against uranium to visualize if any hydrothermal alteration is linked to the mineralization (Fig. 8). Table 4 suggests a combination of chemical and hydrothermal alteration and the former is masked the later because of dominance in surficial environment subsequent to hydrothermal alteration. The correlation coefficient values between different alteration indices and uranium (Table 5) show apparently a combined effect of chemical and hydrothermal alteration. Hydrothermal index gives linear positive trend in contrast to the chemical index which is nonsystematic in nature and thus the grab samples collected from surface is not showing much intense indication of hydrothermal effects.

Now, if the Tummalapalle area is considered, the tables (Table 1, Table 2 and Table 3) show the major oxides, significant trace elements and REE concentrations of the samples. REE concentrations in rock are normalized to a common reference standard, which most commonly comprises the values for chondritic meteorites. The REE are presented in a concentration (1×10^{-6}) vs atomic number diagram in which concentrations are normalized to the chondritic reference value expressed as the logarithm to the base 10 of the value. Concentrations at individual points on the graph are connected by line which is commonly called Masuda-coryell diagram. The data shows quite different pattern. For normalizing REE composite of 12 chondrites (Wakita H et al., 1971) are used (Fig. 9a). However, it has been observed that concentration of many elements in sedimentary rocks in continental platforms around the world is similar as a consequence of mixing through repeated cycles of erosion. This average sediment also has been used as the normalizing value of REE. Here, Post Archaean average Australian sedimentary rock (PAAS) standard (Mc Lennan SM, 1989) are used (Fig. 9b). However, the PAAS may reflect multiple source and shows negative values for some LREE and chondrite normalization are considered to be interpreted the provenance. The single most important factor contributing to the REE content of the clastic sediments is its provenance. Hence, direct interpretation of basement granitoids can be applicable from these REE data. Firstly, negative Eu anomalies are indicative of removal of feldspar from the system. Removal of feldspar from felsic melt by crystal fractionation or partial melting will give rise to negative Eu anomaly in the melt. But, the basement granitoids consists of good proportion of feldspar, which indicates removal of feldspar during transportation of detrital grains as, feldspar have less weathering susceptibility and it can easily be removed and the Gulcheru sediments of the area is compositionally mature enough. Another important observation is enrichment of middle REE compared to HREE

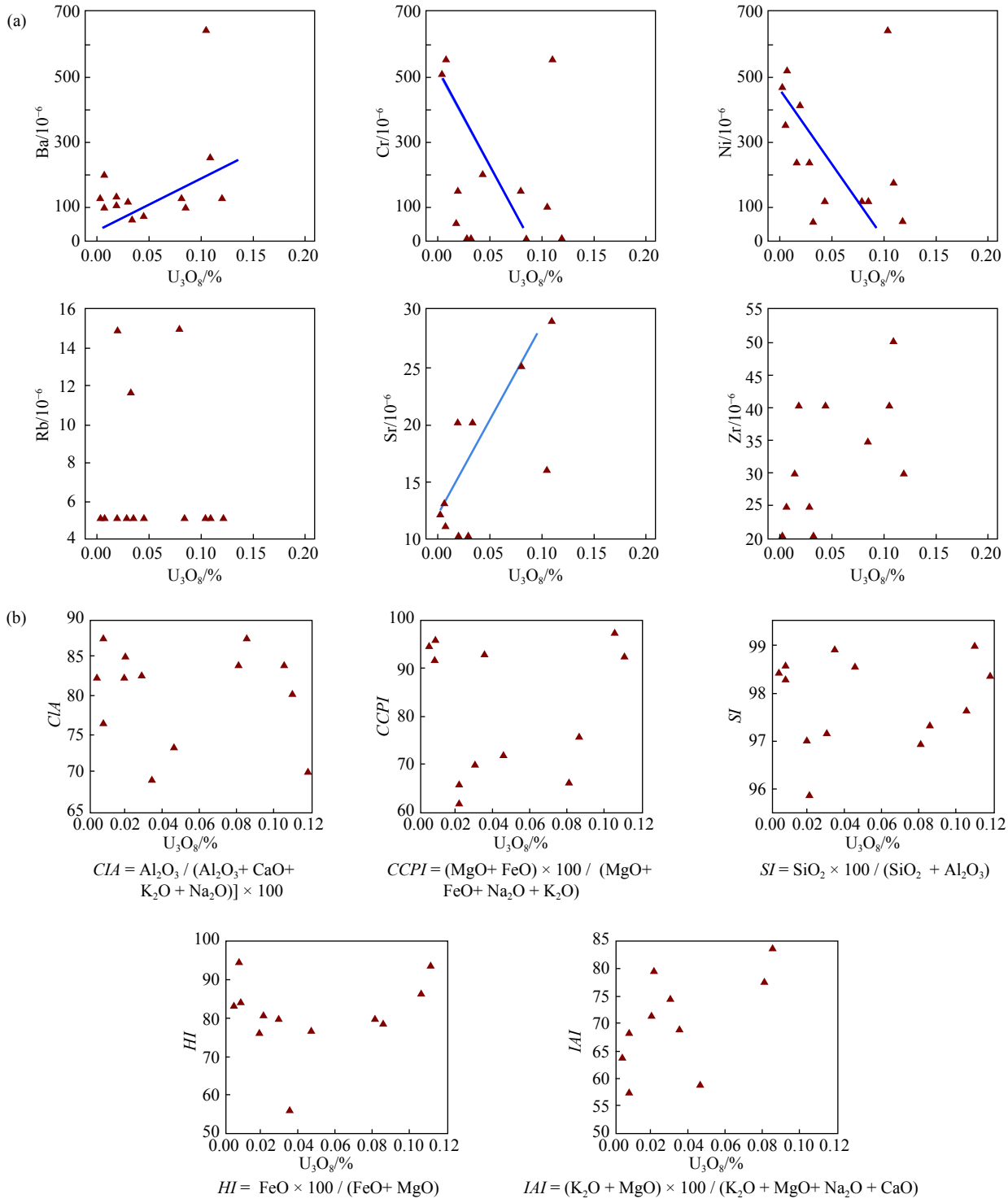


Fig. 8. Geochemical plots. a–Selective trace element plots with respect to uranium; b–different types of alteration indices and their plot with respect to uranium. *CIA* = Chemical Index of Alteration (Nesbitt HW and Young GM, 1982). *IAI* = Ishikawa Alteration Index (Ishikawa Y et al., 1976); *CCPI* = Chlorite-carbonate-pyrite index (Large RR et al., 2001); *HI* = Hashiguchi Index (van Ruitenbeek FJA, 2007); *SI* = Silicification Index (Pirajno F, 2009).

and LREE which perhaps dominantly controlled by hornblende in the system. The MREE are relatively more competent in hornblende in felsic and intermediate liquids and highest partition coefficient are observed between Dy and Er. Therefore, even moderate amount of hornblende (20%−25%) may dominate the bulk partition coefficient for this range of elements and influence the shape of REE pattern. The same effect can also observe with clino pyroxene and sphene to a lesser extent.

Therefore, the REE pattern of the data indicates hornblende rich uraniferous fertile granitoid as source for the Tummalapalle quartzite.

Table 4. Alteration indices of Gulcheru quartzite samples, Ambakapalle area.

Sample. No.	*CIA*	*IAI*	*HI*	*SI*	*CCPI*
ABP-1	69.00	68.80	55.70	98.90	92.90
ABP-2	73.40	58.80	76.40	98.60	71.80
ABP-3	84.00	77.60	79.60	96.90	66.00
ABP-4	70.00	52.70	67.70	98.30	70.70
ABP-5	85.30	79.30	80.40	95.80	65.80
ABP-6	82.90	74.30	79.30	97.10	69.80
ABP-7	82.50	71.20	76.00	97.00	61.50
ABP-8	87.70	84.00	78.40	97.30	75.50
ABP-9	84.00	65.70	86.10	97.60	97.50
ABP-10	82.30	63.80	83.20	98.40	94.40
ABP-11	87.60	68.30	94.40	98.30	95.80
ABP-12	80.50	50.00	93.90	99.00	92.40
ABP-13	76.70	57.10	83.40	98.60	91.60

Table 5. Correlation matrix of uranium and alteration indices, Ambakapalle area.

Data	*CIA*	*IAI*	*HI*	*SI*	*CCPI*	U_3O_8
CIA	1					
IAI	0.6	1				
HI	0.7	−0.1	1			
SI	−0.6	−0.8	−0.04	1		
CCPI	−0.05	−0.4	0.3	0.7	1	
U_3O_8	0.3	−0.05	0.4	0.2	0.5	1

4.2. Role of deformation structures

Role of deformation and associated enrichment of uranium is possibly more significant in Ambakapalle area. The fault zones help uranium bearing fluid to migrate into the structural trap and precipitate the uranium minerals. This structural setting might have provided enough time to react the fluid with receptive host rock. Heat, pressure and fractures have played a combined role in uranium mineralization in Ambakapalle area. The localization of uranium is influenced by E-W fault zone which have provided the pathway for hydrothermal fluids. Intersections of fractures are observed as better locations of uranium anomalies and hence given attention for prospecting the uranium mineralization (Fig 10a). The block movement along fault is characterised as diagonal slip normal fault with a net slip direction parallel to the trace of bedding on the fault plane, which is also called trace slip fault. Therefore, from plan view there is no apparent displacement of litho-contacted across the fault (Fig. 10b). This trace slip fault with respect to the strata is interpreted as the most important structure from uranium mineralization point of view. The surficial manifestation of uranium anomalies are often disturbed and intermittent patches of uraniferous anomalies are seen along the trend of fault (Fig. 11a). The step like slickenside lineations (Doblas M, 1998) are identified as evidence of diagonal sip movement towards east (Fig. 11b).

The uranium occurrences in Tummalapalle area is found along NW-SE striking bedding plane with dip ranging from 12° to 16° due NE. The Formation is affected by a ESE-WSW fracture zone and thus sub-vertical fracture scarp face or the dip section shows apparent linear mineralization trend which is not the actual picture because, the mineralization is not only restricted along fracture trend, but also along the bedding. Therefore, there is no direct role of deformation structures in uranium mineralization.

5. Discussions

5.1. Provenance and depositional environment

Chemical composition of Gulcheru Formation is mostly controlled by the source rock from which the erosion, deposition and diagenetic processes lead to development of this sedimentary rocks. Provenance erosion is controlled by tectonics and finally deposited and preserved portions of the detritus can give insight into the provenance setting. Apart from the major elements it is often observed that trace element geochemistry also can be useful. During transport trace element content increases in clayey portions compared to the quartz rich arenitic portions. Therefore trace element concentration can give ideas on palaeo weathering and erosion time span, topography and distance between the source and deposition area, styles and agents of transportation

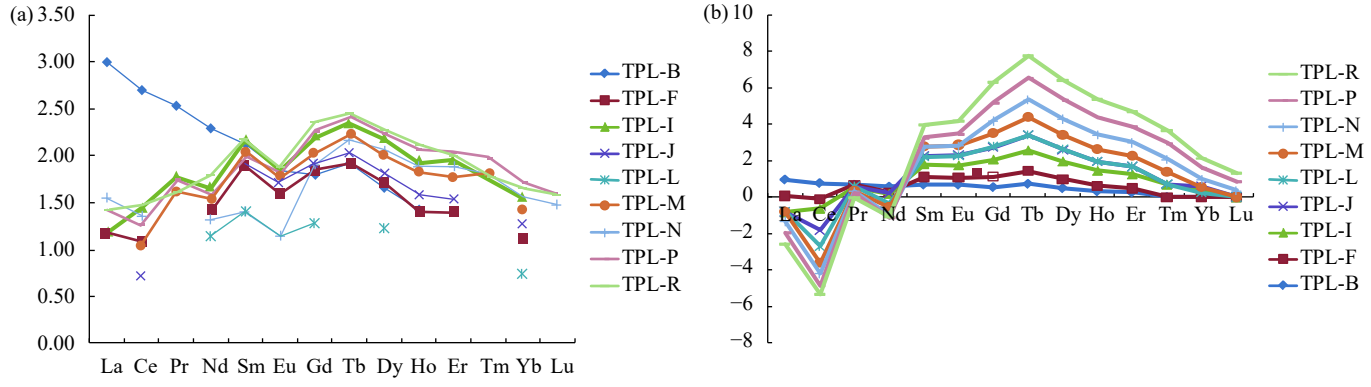
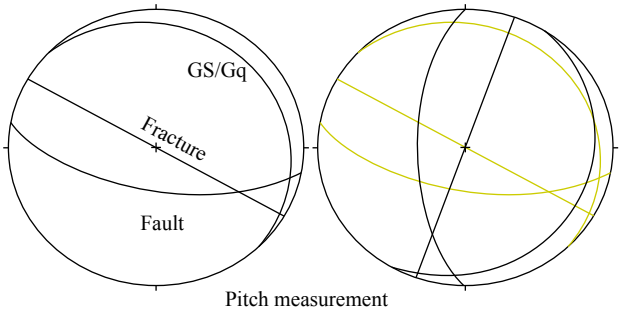


Fig. 9. REE plots with reference to different standards. a–Masuda-coryell diagram of 9 samples composite of 12 chondrites (Wakita H et al., 1971) used for normalizing; b–Masuda-coryell diagram of 9 samples (PAAS) or, post Archaean average Australian sedimentary rock (Mc Lennan SM, 1989) are used for normalizing.

(a)

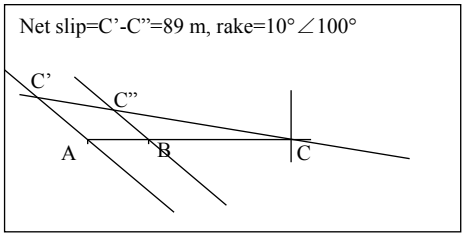
	Strike	Dip	Dip quad
1	100.0	65.0	S
2	315.0	15.0	N
3	300.0	90.0	N

1=fault plane, 2=Gs/Gq contact, 3=vertical fracture.
Rake of trace of bedding and fracture on fault plane is 10°∠100° and 40°∠100° respectively.
Normal trace slip fault w.r.t Formation, southern block downthrown



Pitch measurement





(b)

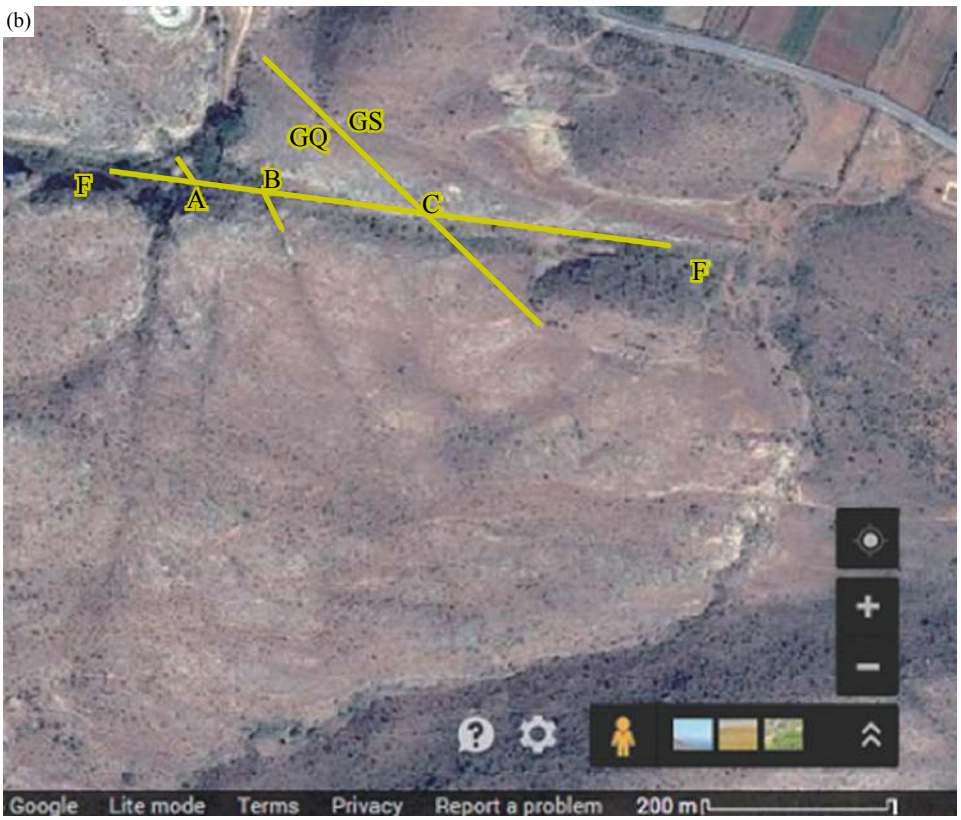


Fig. 10. Structural analysis of Ambakapalle fault zone. a–Net slip calculation with the help stereo net to find rake of trace of bedding and earlier fracture on fault plane and intersection of bedding and fracture on hanging wall and footwall block of the fault. Radioactivity up to 0.9 mR/h has been recorded in footwall block; b–satellite image shows the 100°–280° fault displaced plder NW-SE fracture zone. However, the contact between Gulcheru quartzite (GQ) and Gulcheru shale (GS) is not showing apparent displacement.

etc. In this context inter elemental relationships (Table 6) can also give significant information on depositional processes due to the geochemical association of some elements with similar properties as well as markedly different characteristics with opposite behaviours of some elements. Presently, our aim is to understand the possible palaeo tectonic condition. Since different tectonic condition have their own characteristic provenance set up with typical sedimentation processes, geochemical signatures of sedimentary rocks will be different from back arc, fore arc, inter arc basins, active

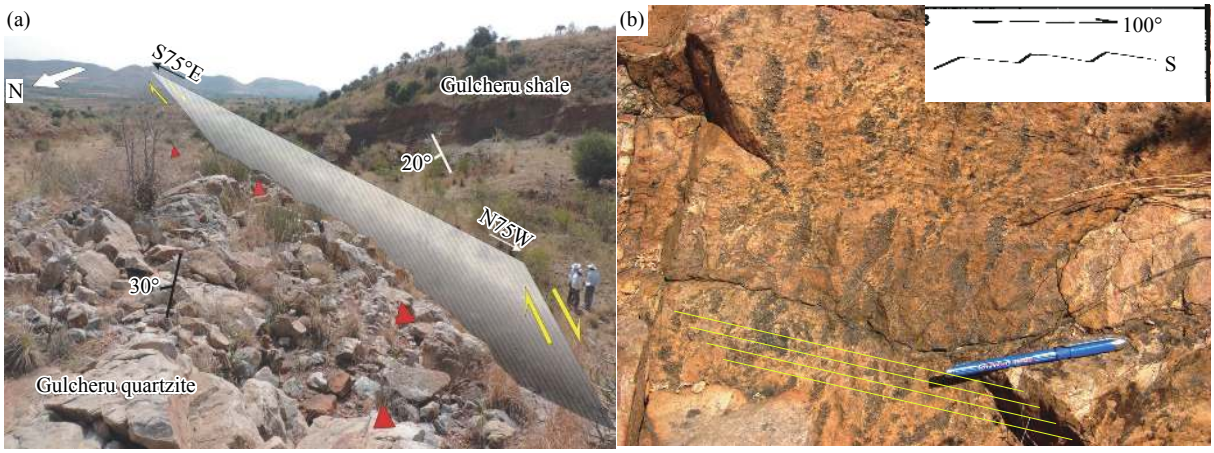


Fig. 11. Regional and outcrop view of fault plane in Ambakapalle area. a–Normal faulting with southern downthrown hang wall block identified from occurrence of younger Gulcheru shale in the downthrown side and older Gulcheru quartzite in the upthrown side at same RL. Dip of the fault plane measured in the field as 70° due south; b–the step like slickenside lineation shows 10°∠100° movement. The direction of motion in the brittle sheared zone is in shear plane/fault plane. This movement must be parallel to fault striations which have been found on 100°–280° fault plane with 10° to 15° pitch due 100°.

Table 6. Correlation coefficient of major oxides and selective trace elements.

Elements	SiO_2	Al_2O_3	TiO_2	Fe_2O_3	FeO	MnO	MgO	CaO	Na_2O	K_2O	P_2O_5	Cu	Co	Ni	V	Cr	Zr
SiO_2	1.00																
Al_2O_3	−0.48	1.00															
TiO_2	−0.09	0.73	1.00														
Fe_2O_3	−0.76	0.05	−0.20	1.00													
FeO	−0.28	0.54	0.09	0.12	1.00												
MnO	−0.51	0.38	0.22	0.29	0.25	1.00											
MgO	−0.33	0.58	0.08	−0.01	0.88	0.43	1.00										
CaO	−0.49	0.22	0.11	−0.05	−0.24	0.29	0.05	1.00									
Na_2O	−0.88	0.70	0.31	0.49	0.39	0.55	0.55	0.50	1.00								
K_2O	0.21	0.30	0.56	−0.35	−0.34	−0.26	−0.20	0.14	0.08	1.00							
P_2O_5	−0.51	0.22	0.12	−0.02	−0.24	0.28	0.04	1.00	0.51	0.11	1.00						
Cu	−0.21	−0.02	−0.18	0.28	0.25	0.33	0.18	−0.15	0.06	−0.49	−0.15	1.00					
Co	−0.76	0.06	−0.27	0.87	0.21	−0.02	0.13	−0.09	0.53	−0.32	−0.06	0.29	1.00				
Ni	−0.76	0.11	−0.36	0.95	0.12	0.26	0.07	−0.14	0.60	−0.28	−0.11	0.29	0.88	1.00			
V	−0.76	0.04	−0.16	0.99	0.06	0.32	−0.06	−0.06	0.50	−0.33	−0.03	0.31	0.85	0.96	1.00		
Cr	−0.64	0.02	−0.19	0.95	0.02	0.22	−0.10	−0.15	0.44	−0.18	−0.13	0.26	0.78	0.96	0.96	1.00	
Zr	−0.56	0.66	0.40	0.01	0.11	0.43	0.36	0.76	0.71	0.32	0.74	−0.12	−0.03	0.08	0	−0.02	1.00

and passive continental margins, collisional or rift settings (Bhatia MR and Crook KAW, 1986).

After plotting the data in the Al_2O_3% versus TiO_2% (Fig. 12a) bivariate discrimination diagram (McLennan SM et al., 1990) to assign the proven anceit is seen that samples of the present study plot in the alkali granite-granite field. Another bivariate TiO_2% versus Ni (10^{-6}) diagram (Fig. 12b) to evaluate source rock composition (Floyd PA et al., 1989) indicate this mature sandstone are derived from acidic igneous rocks. The bivariate plot after Bhatia, 1983 is also used to make out about the possible tectonic setting on the basis of Fe_2O_3, MgO, Al_2O_3, SiO_2 and TiO_2 content (Fig. 12c, d). This plot suggests about passive margin setting. Further, two discriminant functions are calculated from the present data as per the following formula proposed by Bhatia (1983) :

Discriminant function 1 = (−0.0447×SiO_2%) + (−0.972×TiO_2%)+(0.008×Al_2O_3%)+(−0.267×Fe_2O_3%)+(0.208×FeO%)+(−3.082×MnO%)+(0.140×MgO%)+(0.195×CaO%)+(0.719×Na_2O%) + (−0.032×K_2O%) + (7.510×P_2O_5%).

Discriminant function 2 = (−0.421×SiO_2%) + (1.988×TiO_2%) + (−0.526×Al_2O_3%) + (−0.551× Fe_2O_3%) + (−1.610×FeO%) + (2.720×MnO%) + (0.881×MgO) + (−0.907×CaO%) + (−0.117×Na_2O%) + (−1.840×K_2O%) + (7.244×P_2O_5%).

The bivariate plot of the discriminant functions (Fig. 13) also represents passive margin setting. Therefore, the provenance for the Gulcheru Formation is hereby characterized as passive margin.

5.2. Genetic model of uranium mineralization

5.2.1. Ambakapalle area

The Ambakapalle uranium mineralization represents a mechanism of hydrothermal fluid movement along fracture during late orogenic phase. The two opposite events took

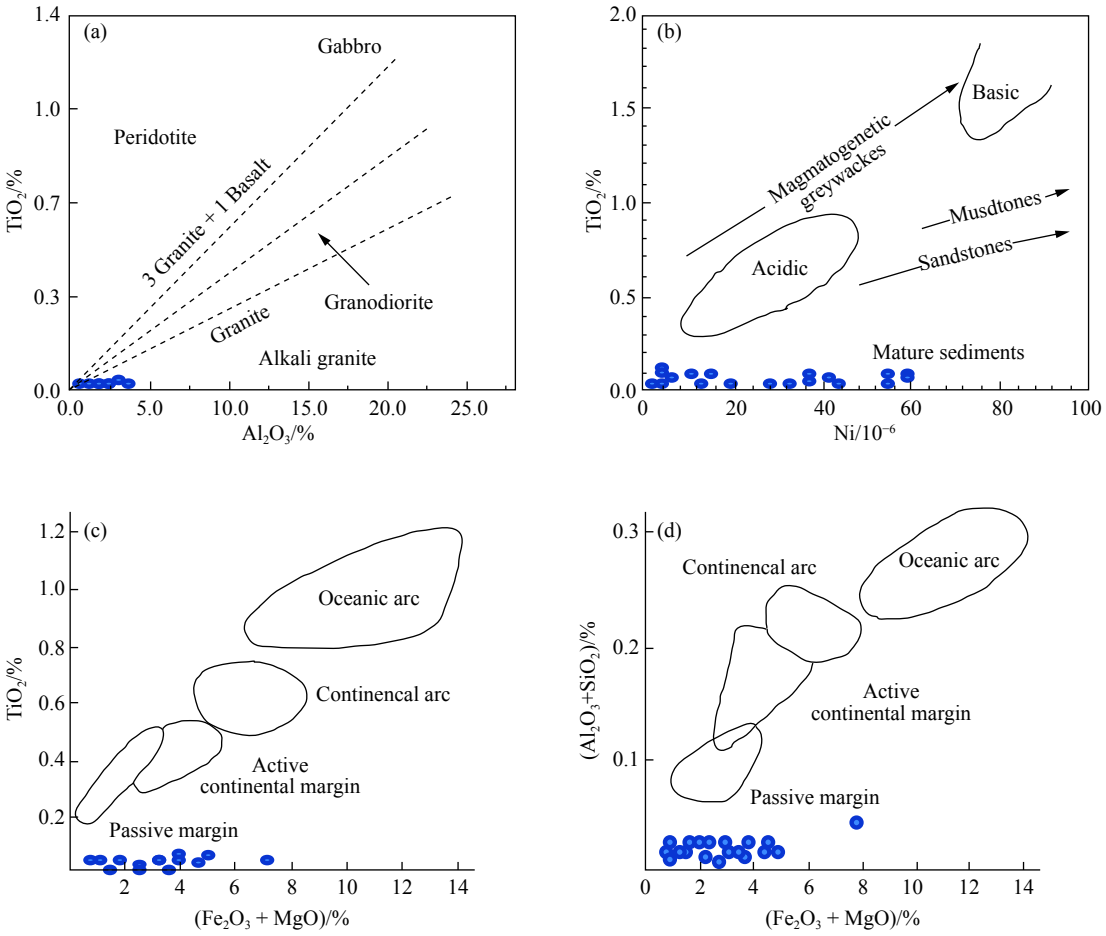


Fig. 12. Geochemical plots for provenance characterization. a–Al_2O_3 versus TiO_2 bivariate discrimination diagram (McLennan SM et al., 1990); b–TiO_2 versus Ni (10^{-6}) diagram (Floyd PA et al., 1989); c–TiO_2 versus Fe_2O_3 + MgO bivariate diagram (Bhatia MR, 1983); d–Al_2O_3 / SiO_2 versus Fe_2O_3 + MgO % bivariate diagram (Bhatia MR, 1983).

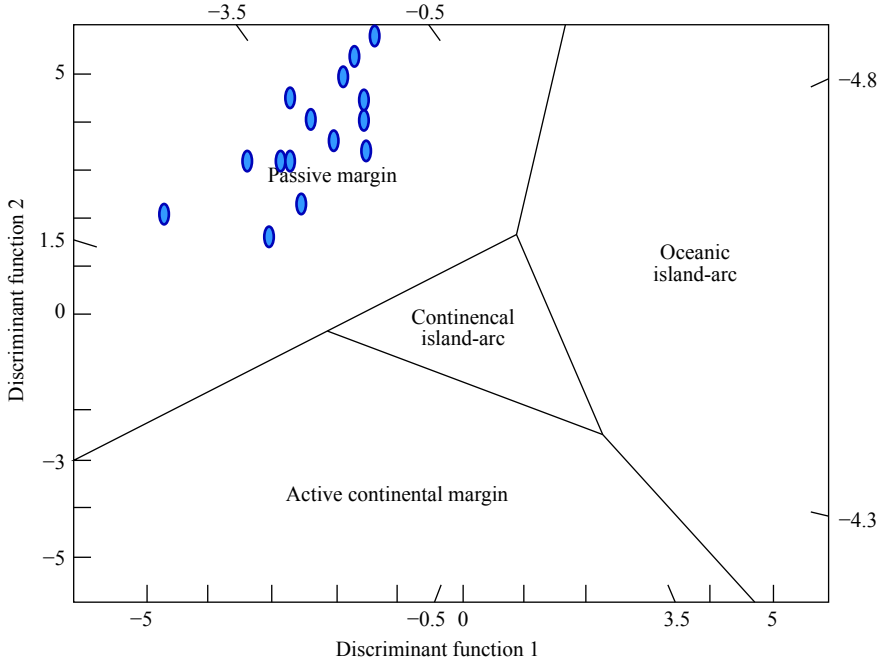


Fig. 13. Bivariate plot of two discriminant functions (Bhatia MR, 1983).

place in this area. The intrusion of mafic dike along the fracture pathway and diagenetic changes of the host sediments. The dyke intrusion produces an additional heat and reductants like pyrites, galena to enhance the uranium holding capabilities. However, diagenesis may generate a remobilization condition with addition or removal of uranium. The fulfilment of requirements like favourable structural setup for tapping the mineralization and presence of ore-bearing fluids in these structures lead to such structurally controlled mineralization. The genetic model (Fig. 14a) shows the 3D visualization of the entire set up. The ore bearing fluids possibly have reacted continuously with the wall rocks and further chemical weathering and alteration at shallow depth have masked the possible deeper features. The iron might have provided electron to uranium for reduction and precipitation. Simultaneously, oxidation of iron due to loss of electron leads to its co-precipitation along fractured wall. This is because of the opposite geochemical properties of iron and uranium. Unlike uranium, iron in ferrous state is soluble and when oxidized to the ferric state it become insoluble and precipitate. Therefore, the Ambakapalle uranium mineralization suggests the initial oxidation of hydrothermal fluids by wall rock elements (Fig. 14b) and also by the mixing of surficial fluid which caused oxidation of uranium. Further, reductents like pyrite, chlorite etc. was provided by later emplaced mafic dyke. Later surficial chemical alteration and complex formation cause the formation of secondary uranium minerals in the vicinity of fault zone.

5.2.2. Tummalapalle area

Tummalapalle quartzite hosts uranium deposited possibly at an oxidation-reduction interface with presence of carbon and/or pyrite as reducing agents. Uranium concentration in this siliciclastic rock is governed by its detritus source, compositional and textural properties and organic activities in the form of microbial mats (Goswami S et al., 2016, 2017a, b). Microbial mat can fix inorganic carbon into its structures by carbon autotrophy process. In addition to this oxygenated ground water has played a key role to leach out uranium from source provenance. At places localized oxydation spotsindicate a condition in which oxidising ground water reacted with rocks and thus dark sandstone have often become reddish through the in situ oxidation of ferrous minerals to ferric oxyhydroxide, a precursor of hematite. These spots are also comprising adsorbed uranium on limonite and goethite. Impermeable or less permeable shale above the Gulcheru quartzite restricts permeability for adequate groundwater migration and prohibiting widespread flushing and dilution of uranium rich fluids. The oxidation potential of ground water decreases due to organic mat and become localised reducing environment, which leads to the precipitation of uranium from solution exhibiting syngenetic sedimentation pattern (Durrance EM, 1986). Therefore the proposed model (Fig. 14c) on uranium system of Tummalapalle area comprises fertile fractured basement granitoids as provenance, sandstone with reducing environment due to cyanobacterial activityas

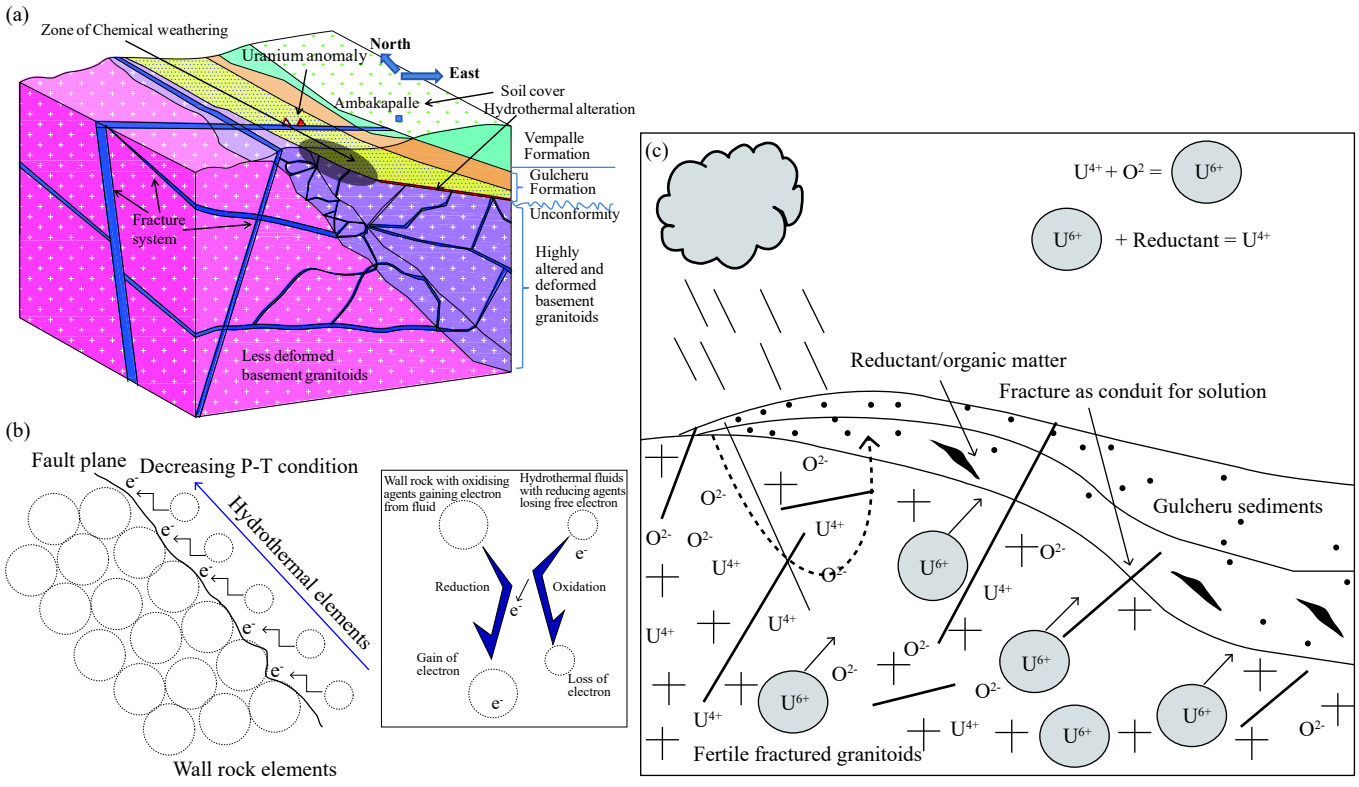


Fig. 14. Diagrams showing the two different setting up. a–Block diagram showing the three dimensional genetic model of Ambakapalle uranium mineralization; b–wall rock alteration and associated uranium mineralization mechanism; c–genetic model showing the mineralisation mechanism in the Tummalapalle area.

the host rock and groundwater as transporting agent and impervious shale as cap for preservation.

6. Conclusion

The two types of uranium mineralization in Ambakapalle and Tummalapalle areas represent different mechanism of enrichment. The Ambakapalle area represents role of fault and associated deformations for enrichment unlike the later which is related to sediment depositional environment and indirect role of organic matter.

Acknowledgement

The authors express sincere gratitude to Shri L.K. Nanda, Director, AMD for encouragement and infrastructure support to publish the work. All the laboratory personnel are thankfully acknowledged.

References

Bhatia MR. 1983. Plate tectonics and geochemical composition of sandstones. The Journal of Geology, 9, 611–627.

Bhatia MR, Crook, KAW. 1986. Trace element characteristics of graywackes and tectonic discriminations of sedimentary basins. Contributions to Mineralogy & Petrology, 92, 181–193.

Dickinson WR, Suczek CA. 1979. Plate tectonics and sandstone composition. AAPG Bulletin, 63(12), 2164–2182.

Doblas M. 1998. Slickenside kinematic indicators. Tectonophysics, 295, 187–197. doi: 10.1016/S0040-1951(98)00120-6.

Dahlkamp FJ. 1993. Uranium Ore Deposits. Springer-Verlag Berlin Heidelberg, New York. ISBN 3–540-53264–1.

Durance EM. 1986. Radioactivity in geology- principles and applications. John Wiley & sons, New York, USA, 1–441.

Floyd PA, Winchester JA, Park RG. 1989. Geochemistry and tectonic setting of Lewisian clastic metasediments from the early Proterozoic Loch Maree group of Gairloch, NW Scotland. Precambrian Research, 45, 203–214. doi: 10.1016/0301-9268(89)90040-5.

Goswami S. 2014. Role of organic matter in Uranium metallogeny in Vempalle Formation. Homi Bhabha National Institute, India, M. Tech. Thesis Report (unpublished).

Goswami S, Mukherjee A, Zakaulla S, Rai AK. 2016. Microbial mat related features in Palaeoproterozoic Gulcheru Formation and their role in low grade Uranium mineralisation. Int J Petrochem Sci Eng, 1(4), 19p. doi: 10.15406/ipcse.2016.01.00019.

Goswami S, Bhagat S, Zakaulla S, Suresh Kumar Rai AK. 2017a. Role of organic matter in Uranium mineralisation in Vempalle Dolostone; Cuddapah Basin, India. Journal of Geological Society of India, 89(2), 145–154. doi: 10.1007/s12594-017-0578-y.

Goswami S, Mukherjee A, Bhattacharjee P, Zakaulla S. 2017b. Primary sedimentary structures and MISS in Gulcheru quartzite along SW part of Cuddapah Basin. Journal of Geological Society of India, 89(5), 511–520. doi: 10.1007/s12594-017-0639-2.

Geological Survey of India (GSI). 1981. Explanatory brochure on geological and mineral map of Cuddapah Basin, 121.

IshikawaY, Sawaguchi T, Iwaya S, Horiuchi M. 1976. Delineation of prospecting targets for Kuroko deposits based on modes of volcanism of underlying dacite and alteration halos. Mining Geology, 26, 105–117.

Jeyagopal AV, Dhana Raju R. 1998. Recognition criteria andsedimentology of dolostone-hosted stratabound uranium mineralisationin Vempalle Formation, Cuddapah basin, Andhra Pradesh, India. *In* : R.N.Tiwari (Ed.) Proceedings of the National Symposium on "RecentResearches in Sedimentary Basins", Indian Petroleum Publishers, DehraDun, 172–179.

Large RR, Gemmell JB, Paulick H. 2001. The alteration box plot: A simple approach to understanding the relationship between the alteration mineralogy and lithogeochemistry associated with volcanic-hosted massive sulfide deposits. Economic Geology, 96, 957–971.

McLennan SM. 1989. Rare earth elements in sedimentary rocks: influence of provenance and sedimentary processes. In. Lipin, B.R., and Mc Kay, G.A. (eds.) Geochemistry and mineralogy of rare earth elements. Reviews in Mineralogy, 21, 169–200.

McLennan SM, Taylor SR, Mc Culloch MT, Maynard JB. 1990. Geochemical and Nd-Sr isotopic composition of deep sea turbidites: crustal evolution and plate tectonic associations. Geochimica Et Cosmochimica Acta, 54, 2015 –2050. doi: 10.1016/0016-7037(90)90269-Q.

McLennan SM, Taylor SR. 1991. Sedimentary rocks and crustal evolution revisited: tectonic setting and secular trends. The Journal of Geology, 99, 1–21. doi: 10.1086/629470.

Nagaraja Rao BK, Rajurkar ST, Ramalingaswami G, Ravindra Babu B. 1987. Stratigraphy, structure and evolution of Cuddapah Basin. In: Radhakrishna, B.P. (Ed.), Purana Basins of peninsular India. Mem. Geol. Soc. India, 6, 33–86.

Nesbitt HW, Young GM. 1982. Early Proterozoic climates and plate motions inferred from major element chemistry of lutites. Nature, 199, 715–717.

Parihar PS, Rao JS. 2012. Cuddapah basin - a uanium province. Exploration and Research for Atomic Minerals, 22, 1–19.

Pirajno F. 2009. Hydrothermal processes and mineral systems. Springer Science & Business Media, ISBN 140208613X, 9781402086137.

Ramakrishnan M, Vaidyanadhan R. 2008. Geology of India (Volume 1). Geological Society of India. Bangalore.

Rai AK, Zakaulla S, Jeygopal AV, Vasudeva Rao, Naghbhushna JC, Vardaraju HN. 2002. Uranium Mineralisation in Southwestern part of Cuddapah Basin, Andhra Pradesh. Exploration and Research for Atomic Minerals, 14, 79–94.

Roser BP, and Korsch RJ. 1986. Determination of tectonic setting of sandstone-mudstone suites using SiO_2 content and K_2O/Na_2O ratio. The Journal of Geology, 94, 635–650. doi: 10.1086/629071.

Roser BP, Korsch RJ. 1988. Provenance signatures of sandstone-mudstone suites determined using discriminant function analysis of major element data. Chemical Geology, 67, 119 –139. doi: 10.1016/0009-2541(88)90010-1.

van Ruitenbeek FJA. 2007. Hydrothermal processes in the Archaean: new insights from imaging spectroscopy. ITC dissertation; ITC, Enschede, 148.

Wakita H, Rey P, Schmitt RA. 1971. Abundances of the 14 rare-earth elements and 12 other trace elements in Apollo 12 samples: five igneous and one breccia rocks and four soils. Proc. 2nd Lunar Sci. Conf. Pergamon press, Oxford, 1319–1329.